Urban Climate 36 (2021) 100787

Contents lists available at ScienceDirect

Urban Climate

journal homepage: www.elsevier.com/locate/uclim

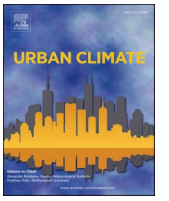

Climate change and infrastructure risk: Indoor heat exposure during a concurrent heat wave and blackout event in Phoenix, Arizona

Brian Stone Jr. [a,*], Evan Mallen [a], Mayuri Rajput [b], Ashley Broadbent [c], E. Scott Krayenhoff [d], Godfried Augenbroe [b], Matei Georgescu [c]

[a] School of City and Regional Planning, Georgia Institute of Technology, Atlanta, GA, 30332, USA
[b] School of Architecture, Georgia Institute of Technology, Atlanta, GA, 30332, USA
[c] School of Geographical Sciences and Urban Planning, Arizona State University, Tempe, AZ, 85287, USA
[d] School of Environmental Sciences, University of Guelph, Guelph, ON, N1G 2W1, Canada

A B S T R A C T

Concurrent with a rapid rise in temperatures within US cities, the frequency of regional electric grid system failures is also rising in recent decades, resulting in a growing number of blackouts during periods of extreme heat. As mechanical air conditioning is a primary adaptive technology for managing rising temperatures in cities, we examine in this paper the impact of a prolonged blackout on heat exposure in residential structures during heat wave conditions, when air conditioning is most critical to human health. Our approach combines a regional climate modeling system with a building energy model to simulate how a concurrent heat wave and grid failure event impacts residential building-interior temperatures across Phoenix. Our results find a substantial increase in heat exposure across residential buildings in response to the loss of electrical power and mechanical cooling systems, with such an event potentially exposing more than one million residents to hazardous levels of heat. We further find the installation of cool roofing to measurably lower the risk of extreme heat exposure for residents of single-story structures.

1. Introduction

Extreme heat is among the leading causes of weather-related mortality in the US (Shindell et al., 2020; Dixon et al., 2005; Berko et al., 2004), and the environmental hazard most confidently projected to worsen with climate change (Parry et al., 2007). Heat wave activity is increasing rapidly in the US: the average incidence in cities has increased 20% per decade since 1960, and the duration and intensity of heat waves have increased in tandem (Habeeb et al., 2015). Despite this, heat-associated mortality in the US has declined over time, partly due to the increasing prevalence of mechanical air conditioning (AC) (Davis et al., 2003; Petkova et al., 2014; Hondula et al., 2015), arguably the most effective measure for preventing heat exposure (Kovats and Hajat, 2008).

With an increasing reliance on mechanical cooling for heat management comes a growing potential for significant adverse impacts if electrical power is not available, particularly in cities where urban heat islands and other factors heighten climate change vulnerability (Patz et al., 2005). As a result of both extreme weather and increased demand, the number of electric grid failures events has risen steadily. Fig. 1 reports annual trends in the *Systems Average Interruption Duration Index* (SAIDI), a measure of the annual average period (in minutes) of power loss per residential power utility customer. Presented for all US power utilities, the duration of electric grid failure increased by approximately 40% between the 2013–14 and 2017–18 periods, revealing a rising potential for concurrent heat wave and blackout events. Climate change, by increasing summertime energy demand and stressing grid reliability, is

* Corresponding author.
E-mail address: stone@gatech.edu (B. Stone).

https://doi.org/10.1016/j.uclim.2021.100787
Received 8 May 2020; Received in revised form 3 October 2020; Accepted 24 January 2021
Available online 11 February 2021
2212-0955/© 2021 Elsevier B.V. All rights reserved.

likely to further increase the risk of blackouts over time (Van Vliet et al., 2012).

Electric grid failures can have dramatic public health effects, as demonstrated during a combined derecho and heat wave event in the eastern US in June 2012. More than 4 million lost power as temperatures exceeded 38 °C. While there is no comprehensive estimate of health effects, press accounts in Maryland and Virginia alone reported at least 30 heat-related fatalities. This was likely a marked underestimate: an analysis of the two-day August 2003 New York City blackout identified a 28% increase in all-cause mortality (Anderson and Bell, 2012). Assuming a proportional impact, the 2012 blackout event may have caused hundreds of excess deaths.

Despite the potential for significant health impacts, only limited work to date has focused on heat exposures resulting from electric grid system failures during periods of extreme heat (Sailor et al., 2019). In this study, we assess the extent to which a concurrent heat wave and blackout event in Phoenix, Arizona (USA), elevates simulated building-interior heat exposures under different scenarios. Situated in the hot and arid Southwest climate region of the US, and with a rapidly growing population of more than 1.6 million residents (US Census Bureau, 2020), Phoenix represents one of the most extreme thermal environments for a major urban area in North America. Scenarios of interest include the range of exposures across different building types, including both single family and multifamily, in response to two urban heat management strategies (high albedo roofing and street tree planting), and within relatively hotter and cooler zones of Phoenix. Three questions, in particular, are addressed by this study: 1. How do building-interior heat exposures change during a concurrent heat wave and blackout event for different residential building types? 2. How effective are urban heat management strategies in reducing building-interior heat exposures? 3. How do building-interior temperatures vary with the spatial intensity of the urban heat island?

2. Methods

Our research approach combines a regional climate modeling system with a building energy model to simulate how a concurrent heat wave and grid failure event would impact residential building-interior temperatures across Phoenix. A core observation underlying our approach is that the residential structure mediates the effects of environmental, engineering, and behavioral hazards associated with heat on human health outcomes. Through the combination of a regional climate and a building energy model, we assess the effectiveness of specific adaptations to reducing building-interior heat exposure and potentially lessen heat-related health impacts.

An inventory of single-family and multi-family residential buildings across Phoenix identified a limited number of representative

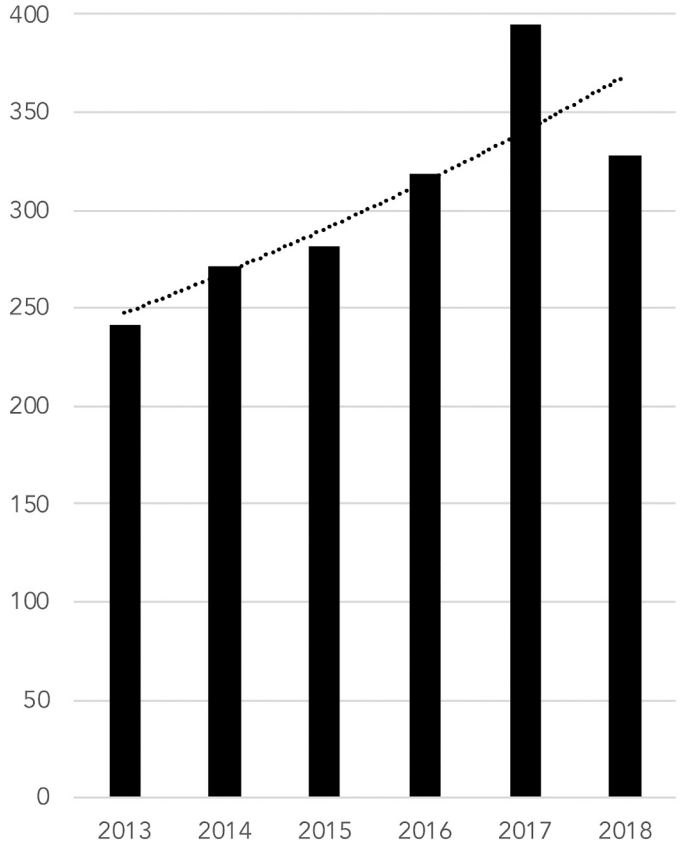

Fig. 1. Average annual Systems Average Interruption Duration Index (SAIDI) for US power utilities: 2013–18. The y-axis reports minutes of electrical service interruption. Source: USEIA, 2019.

building structure types. A tax parcel attribute dataset from the City of Phoenix enabled the classification of every residential structure based on the number of residential units, floor area, number of stories/building height, exterior construction materials, and insulation properties (based on the year of construction) (City of Phoenix, 2019). Based on this inventory, residential structures were grouped into discrete sets of building types for which building energy modeling prototypes were developed. The development of class prototypes enabled building-interior temperature and humidity conditions to be modeled in response to changing ambient conditions and the availability/operability of mechanical cooling and ventilation systems, as simulated through a regional heat wave and grid failure modeling process, described below.

Regional climatic conditions during a historical heat wave event were simulated with the Weather and Research Forecasting (WRF-ARW) system (Skamarock et al., 2008). Three regional climate scenarios were developed for this study, including a contemporary climate scenario consistent with a recent heat wave event, a scenario in which high albedo or "cool" roofs are assumed to be installed on all structures, and a street tree scenario through which 50% of all road surfaces are assumed to be overlaid by tree canopy. These three WRF simulations are referred to as the BASE, COOL, and TREE scenarios, respectively.

The WRF simulations made use of a multi-layer urban canopy model called the Building Environment Parametrization (BEP) (Martilli et al., 2002). Importantly, the BEP scheme resolves meteorological variables at "street-level," meaning that the cooling impacts of interventions are captured at this level (Broadbent et al., 2020). High-resolution (1 km grid spacing for the innermost domain) two-way coupled BEP/WRF-ARW (hereafter WRF) simulations were performed using a nested grid configuration, permitting the downscaling of the large-scale synoptic flow from the coarsest outer grid to the finest inner grid across the Phoenix region. The Integrated Climate and Land Use Scenarios (ICLUS) dataset for 2010 (Bierwagen et al., 2010), available from the US Environmental Protection Agency for the conterminous US, was used to represent the contemporary urban landscape. ICLUS classes were mapped to the WRF domain, ranging from a rural/exurban designation, to medium intensity, and to high-intensity/commercial development, using an approach similar to a recent continental US hydroclimatic examination of urban expansion impacts (Georgescu et al., 2014; Krayenhoff et al., 2018). For a full description of the WRF model setup and input datasets used in this study please refer to Broadbent et al. (2020).

Due to our interest in extreme temperatures, we identified and ranked extreme heat wave events in recent Phoenix history (see Broadbent et al., 2020). Heat waves were identified as periods of five or more days where the 97.5th percentile daily average air temperature over the period 1980–2009 was exceeded. This technique of heat wave selection based on a contemporary probability distribution of daily average air temperatures resulted in 10 such events (each lasting at least 120 h) since 1979 for the Phoenix metropolitan area. For the BASE scenario, we selected the most intense of these heat wave events, occurring over July 18–25, 2006, as intense heat waves in the contemporary period are likely to become more common in future time periods (Habeeb et al., 2015).

To assess the extent to which WRF simulations approximate observed meteorology, model output was compared to observations of temperature and precipitation from the Maricopa County Air Quality Department (MCAQ), Arizona Meteorological Network (AZMET), and the MesoWest Database, which contains daily observations of minimum, maximum, and mean temperature. The monthly evolution of WRF simulated 2-m temperatures corresponded well to Phoenix observations. The root mean square error (RMSE) for urban and fringe sites (airports) was 2.6 and 2.7 °C, respectively, with the model found to have a warm bias during the day and a cool bias during the night (please see for more details on model validation Broadbent et al., 2020). Based on these findings, the external air temperature forcing from WRF that drives the building-interior climate modeling may be slightly too warm during the day and slightly too cool at night. In general, over the city, WRF's cool nighttime bias is stronger than the warm daytime bias.

The COOL scenario was simulated in WRF by increasing the roof surface albedo of all rooftops from 0.16 to 0.88. An albedo of 0.88 was based on the "SOLARFLECT" roof coating product, included in the US Environmental Protection Agency's Energy Star roof product list (USEPA, 2020). Among commercially available roofing products this is a near maximum obtainable roof albedo treatment.

For the TREE scenario, street tree canopy was represented as a layer of foliage within the canyon space above street level between 5 and 10 m (midsize trees), amounting to a leaf area index (LAI) of 1.0 within the canyon space. Foliage is assumed to have a spherical leaf angle distribution and a clumping coefficient of 0.70, which corresponds to a 50% plan area coverage of streets by tree crowns, each with a crown-scale LAI of 1.8 m^2. We assume that tree crowns are approximately spherical and that the dominant foliage clumping scale corresponds to the distribution of tree crowns within the street (Krayenhoff et al., 2020).

All solar radiation is assumed to be direct in the BEP urban canopy model, and therefore the Beer-Bouguer-Lambert law is applied to intercept incoming radiation as a function of solar zenith angle. Additional penetration of solar radiation onto the urban surfaces below the tree canopy due to forward scattering (transmission) by leaves is modeled with the Goudriaan (1977) modification to the extinction coefficient in the Beer-Bouguer-Lambert law (Campbell and Norman, 1998), assuming a leaf absorptivity of 0.50. This general approach to the interaction of trees with solar radiation is a simplification of the interception and scattering of direct shortwave radiation applied in the BEP model (Krayenhoff et al., 2020; Krayenhoff et al., 2014). Here, street tree impacts on local climate are represented solely in terms of their provision of shade to underlying streets and nearby surfaces (but not direct shading of residential structures) and a corresponding assumption that this energy is converted solely to transpiration. Note that this assumption effectively assumes maximum potential tree transpiration from an energy balance standpoint, because heating of the urban canopy atmosphere that would otherwise accrue from leaf sensible heat flux is assumed to be directed toward transpiration in the current approach. As a result, any simulated cooling effects of our TREE scenario are representative of maximum potential cooling.

We made use of a finite element modeling (FEM) approach for building performance simulations and to predict the environmental conditions inside different types of single and multi-family residential structures across Phoenix (Rajput and Augenbroe, 2019; Li et al., 2008; Augenbroe et al., 2008). The FEM approach modifies the widely used US Department of Energy *EnergyPlus* model (Crawley et al., 2000) to more fully represent building-interior climate conditions. The FEM discretizes the building fabric and internal zones as a mesh of nodes and elements where the nodes represent state variables (temperatures) and the elements represent modes of heat transfer

(conduction, convection, radiation and airflow). This model is handcrafted for each prototype on MATLAB to increase the robustness of the large number of simulations that are required for each grid of the city.

A single warm-up simulation cycle of three full years is performed to obtain the initial temperatures of all the nodes for each prototype with Typical Meteorological Year (TMY) data. Warm-up ensures that temperatures of all surfaces are at an equilibrium before the core simulation starts. Warm-up stops at the date and time of the historical heat wave period. Beyond this timestep, iteration for each WRF grid cell takes over the weather control and each prototype is simulated for the microclimate of that grid. This process is repeated for each 1-km WRF grid cell in Phoenix, and hourly temperatures for the three residential structures are obtained for the full period of simulation.

This modeling approach facilitates simulation of the internal environmental conditions of any residence in any given urban context under given weather scenarios and mechanical climate control systems. Building-interior climates were simulated in response to the three regional climate simulations, including the BASE, COOL, and TREE scenarios. As the FEM approach is designed to respond directly to the ambient variable output by the WRF model, including temperature, humidity, and windspeed, the building energy simulations were driven both by the climate and electric grid operability scenarios. For the COOL scenario, FEM is modified to account for high albedo roof materials.

For this analysis, we simulated interior temperatures in buildings representative of typical residential structures in the Phoenix study area. The residential structure types for which building-interior climates were simulated included 1-story single family houses ("1-Story SF"), 2-story single family houses ("2-Story SF"), and 3-story multifamily apartment buildings ("Apartment"). Standard model prototypes for each of these three residential building types were obtained from the US Department of Energy's *EnergyPlus* whole building simulation model and are constructed based on parameters from the USDOE Building Energy Codes Program (USDOE, 2017). Model prototype parameters, including building age, size, construction materials, and insulation values, are reflective of the local residential building stock in Phoenix. It is estimated that 87% of all residential structures in Phoenix meet or exceed the 2006 International Energy Conservation Code requirements (Mendon et al., 2013). Our approach makes use of higher thermal mass parameters (e.g., lower insulation values) for older buildings that fail to meet the IECC 2006 code.

Each residential structure in Phoenix was classified into one of these three standard building prototypes with the aid of parcel tax data reporting the number of stories and the number of housing units per structure (City of Phoenix, 2019). No structures are assumed to have a basement and all consist of stucco (cement based) siding. For each structure type, interior temperatures in a single, ground-level room are reported. Our simulations assume that building windows are open for ventilation only if doing so would lower indoor temperatures.

As noted above, the WRF and FEM models were run for a historical heat wave event in Phoenix, occurring over the period of July 18–25, 2006. We used ERA-interim reanalysis data during this period to set the boundary conditions for the WRF model (NCAR, 2016), which then provided a full array of ambient meteorological inputs for simulating building-interior climates through FEM. We present simulated building-interior temperatures based on city-wide averages across Phoenix, as well as for relatively hotter and cooler zones within the city, to better understand how building-interior conditions vary spatially with ambient conditions.

To simulate a grid failure event, we assume that all power is lost across the full municipal area of Phoenix at 12:00 am (MST) on the third day of the 8-day heat wave and not restored for a full 5-day period, to allow sufficient time for buildings to dissipate residual cooling from mechanical air conditioning. Driven by the ambient conditions provided by WRF, FEM was run for the 1-Story SF, 2-Story SF, and Apartment structures in every 1-km climate model grid cell in which these structures are found. Two mechanical air

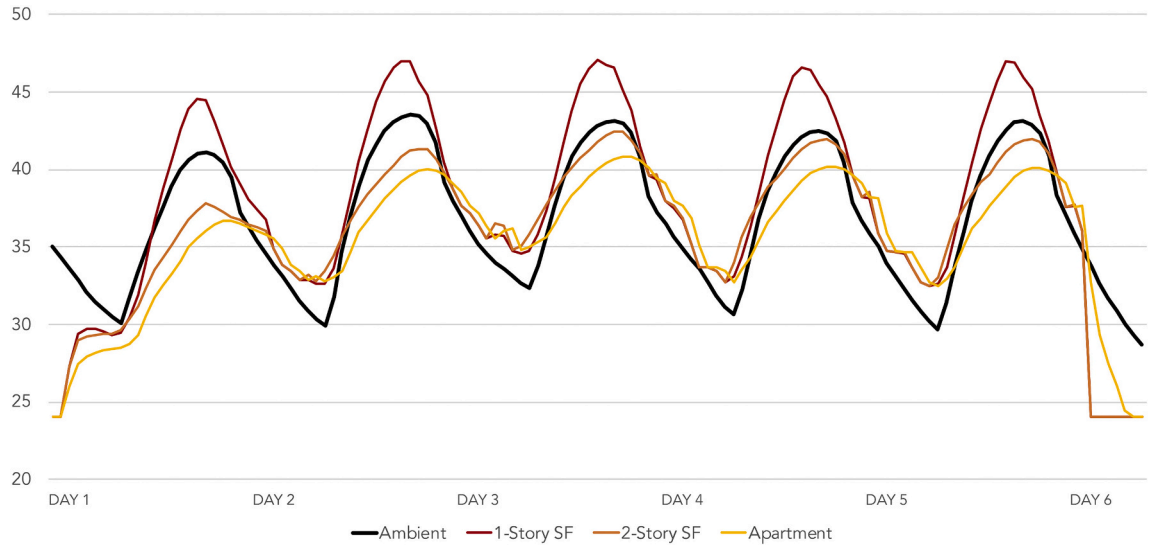

Fig. 2. Simulated average hourly ambient and building-interior temperatures (°C) during a historical heat wave event (July 18–25, 2006) with mechanical air conditioning assumed inoperable for a 5-day period.

conditioning scenarios were simulated for each building type (100% operational AC and 0% operational AC) and in response to the three environmental scenarios: BASE, COOL, and TREE.

3. Results

Hourly ambient and building-interior temperatures for the full 5-day period of concurrent heat wave and blackout conditions are presented in Fig. 2. At the start and conclusion of the blackout simulation, all structures are assumed to have fully operational mechanical air conditioning with a fixed thermostat set-point of 24 °C. Following power loss, significant variability is found among the three building types, with 1-Story SF structures exhibiting building-interior temperatures higher than ambient temperatures throughout most of the period of power loss. Multistory houses and apartment buildings are found to be as much as 5–7 °C cooler than single-story structures during daylight hours, with temperatures in single-story structures matching or falling slightly below multi-story structures during the night.

Loss of electric power during the heat wave event was found to increase late afternoon building-interior temperatures by more than 15 °C across each building type relative to a thermostat set-point temperature of 24 °C when cooling systems are fully operational (Fig. 3; please see Table S1 for detailed temperature values). The greatest increase in heat exposure was experienced by 1-Story SF structures, where average daily maximum building-interior temperatures were found to be 45.5 °C, which exceeded the city-wide average daily maximum ambient temperature of 42.8 °C. With an enhanced capacity to dissipate heat between floors, conditions on the ground level of 2-Story SF and Apartment structures were measurably cooler than single-story houses, with temperatures averaging about 42 and 40 °C, respectively. 1-Story SF family structures in Phoenix tend to be older than 2-Story SF homes and Apartment buildings, with lower average insulation values in walls and ceilings, which contributes to higher building-interior heat exposures during the day.

Building-interior temperatures at night were less variable, with single and multi-story structures found to range between 8.5 and 9 °C warmer than the set-point temperature. With less interior volume to cool off in the evening, 1-Story SF structures were found to be marginally cooler or equivalent to multi-story structures at night. Apartment buildings exhibit lower maximum and minimum temperatures than multi-story houses due the benefits of shared walls for reducing solar gain during the day.

Are urban heat management strategies effective in moderating building-interior heat exposures during a blackout event? Recent work has demonstrated substantial reductions in ambient temperatures resulting from modeled enhancements in surface albedo and tree cover (Stone et al., 2019; Santamouris et al., 2017; Middel et al., 2015). Whether such urban heat management strategies can additionally limit indoor heat exposures for individuals lacking mechanical cooling or during grid failure events is an important question. To assess this potential, we simulated building-interior temperatures during blackout conditions in response to widespread use of cool roofing and street tree planting across Phoenix.

As presented in Fig. 4, cool roofs were found to offer large cooling benefits to maximum building-interior temperatures during

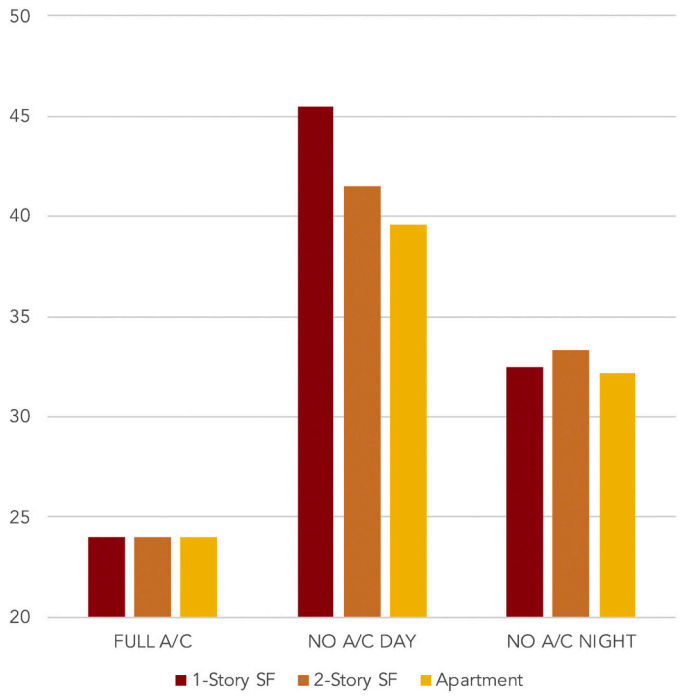

Fig. 3. Average maximum (Day) and minimum (Night) building-interior temperatures during the 5-day heat wave by structure type and AC scenario.

blackouts for 1-Story SF structures, and only moderate cooling benefits for multistory structures. Under the COOL scenario, the average late afternoon temperature for single-story structures was found to be more than 4 °C cooler during blackout conditions than houses with conventional roofs, while cool roofs on 2-Story SF and Apartment structures were found to yield cooling benefits of 0.5 and 0.4 °C, respectively. Cool roofs were found to have only limited (< 0.5 °C) benefits for building-interior temperatures a night.

The widespread planting of street trees, also presented in Fig. 4, was found to have modest (~0.5 °C) and roughly equivalent cooling effects on maximum building-interior temperatures across single and multistory structures. While comparable to the influence of cool roofs on multistory structures, the more modest effects of street tree planting on single story structures relative to the COOL scenario is likely attributable to the degree to which each intervention modifies the performance of the building envelope. Modification of the roof albedo through the COOL scenario directly offsets solar gain by the building structure, with the greatest cooling benefits realized by structures with a higher roof area-to-building volume ratio. Street tree planting, by contrast, entails an intervention that is not integrated into the building structure or even located immediately proximate to the structure. As a result, street trees indirectly reduce building-interior temperatures through their effects on ambient thermal conditions, while cool roofs both reduce ambient temperatures and directly offset solar gain on the building envelope. Street tree planting was also found to have only modest effects on building-interior temperatures at night (< 0.5 °C).

A final question of interest concerns the extent to which spatial location within the urban area elevates building-interior heat exposure. Are residents within the hottest zones of the city more at risk to building-interior heat exposures during blackout conditions than those within cooler zones? As illustrated in Fig. 5, late afternoon temperatures during the heat wave are maximized around the central business district (CBD), due both to moderately lower elevations than north Phoenix (~150 m) and a greater intensity of development, which enhances urban heat island formation. To understand the extent to which elevated ambient temperatures influence building-interior exposure to heat, we examined indoor climates for 1-Story SF houses within the five hottest and five coolest WRF grid cells in which each of the three residential structures types is found. Fig. 5 highlights these grid cells and reports the differences in average maximum and minimum temperatures during the heat wave period. On average, maximum ambient temperatures in the hottest zones are found to be 2.4 °C greater than in the cooler zones, while minimum temperatures are found to vary by 1.5 °C.

As presented in Fig. 6, indoor heat exposure across all structure types is not found to be highly responsive spatial location within the urban heat island. Under the BASE scenario, late afternoon building-interior temperatures are approximately 0.5 °C lower in the coolest zones of the city relative to the hottest zones – much lower than the 2.4 °C difference in ambient temperatures. This differential remains relatively constant across the building types for the COOL and TREE adaptation scenarios.

An examination of diurnal building performance suggests an explanation for this relative consistency in building-interior climates across hotter and cooler zones of the city. Table 1 details average maximum (Day) and minimum (Night) temperatures in hotter and cooler zones over the 5-day heat wave, for both ambient and building-interior conditions. For all structure types, the range of building-interior temperatures is more narrow than that of ambient temperatures, resulting in a negative differential between building-interior and ambient diurnal ranges.

Derived from the last row of Table 1, the average diurnal range for structures in cooler zones (unshaded columns) is found to be 3.6 °C less than the ambient range, while residential structures in hotter zones (gray columns) experience an average range that is 4.8 °C less than the ambient range. This more narrow diurnal range in both cooler and hotter zones indicates that the building envelope is moderating temperature extremes during the course of the day, effectively insulating inhabitants from the highest and lowest

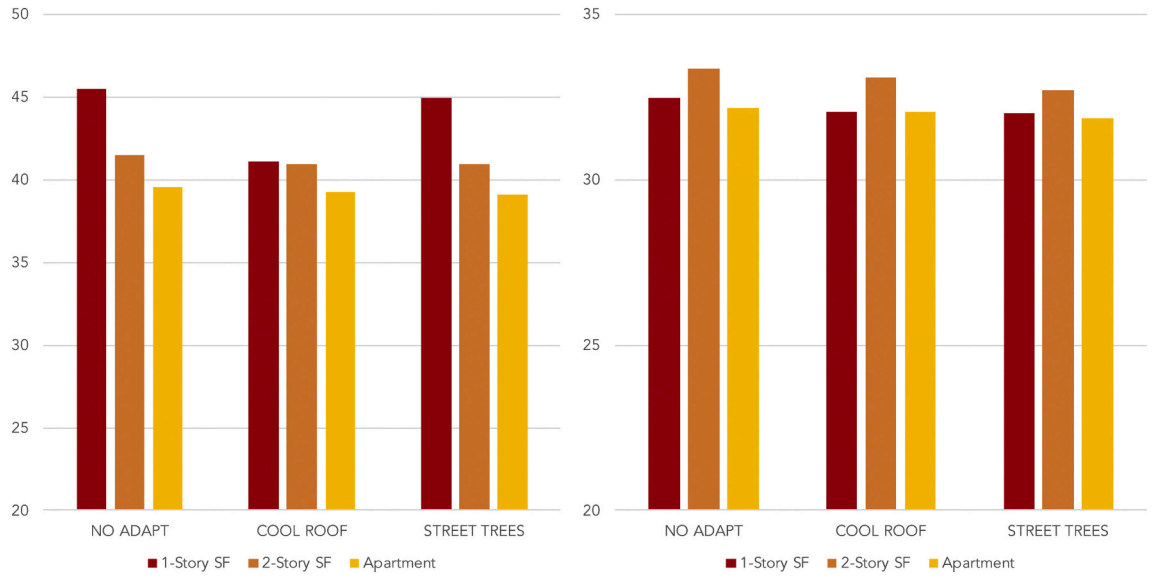

Fig. 4. Results of COOL and TREE adaptation scenarios on average daily maximum temperatures (left panel) and average daily minimum temperatures (right panel) by structure type.

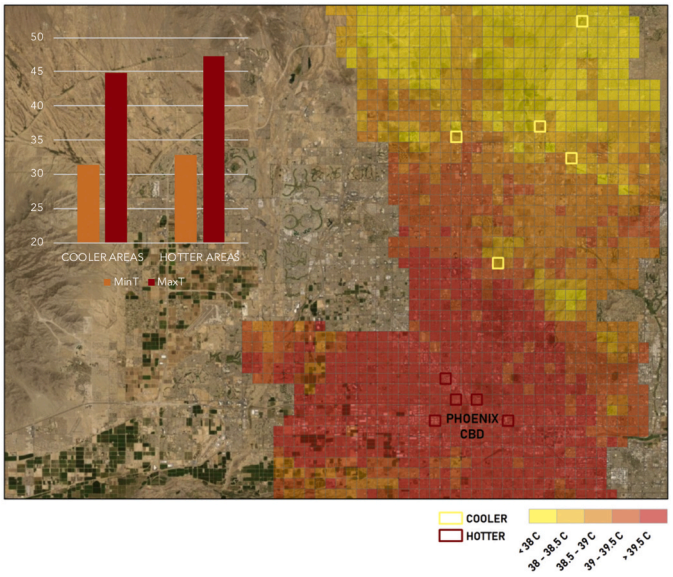

Fig. 5. Average daily maximum and minimum ambient temperatures in hotter and cooler zones of the Phoenix study area during the 5-day heat wave. Highlighted hot and cool areas were selected based on the mean daily average temperature during the heat wave period and the presence of all three residential structures, including 1-Story SF, 2-Story SF, and Apartment buildings. Bar chart reports average maximum and minimum ambient temperatures in the highlighted grid cells over June 20–24, 2006.

ambient temperatures. For buildings in the hottest zones of the city, this negative differential between ambient and building-interior diurnal ranges is greater than found in cooler zones, suggesting that residential structures in hotter zones are increasingly effective in moderating ambient temperatures as these temperatures become more extreme. The result is a less pronounced difference in building-interior climates between hot and cool zones of the city relative to ambient conditions.

4. Discussion and conclusions

An increasing trend toward electric grid disruptions in the United States represents a growing health risk to urban populations as warm season temperatures continue to rise in response to both global (the greenhouse effect) and regional (the urban heat island effect) climate change phenomena. Through this study, we have sought to better understand how heat exposures during a simulated electric grid failure event in Phoenix, Arizona – among the hottest urban climates in the US – may intensify within residential structures. By simulating these effects during a historical heat wave event, we are able to estimate both potential present-day exposures during periods of extreme heat, as well as what is projected to become a more commonly experienced range of temperatures in future periods.

Our findings suggest a high level of risk from building-interior heat exposures during periods of extreme heat and electric grid system inoperability, as well as for households with non-continuous access to mechanical air conditioning due to economic insecurity. While recent Census data finds more than 98% of Phoenix households to report access to central or window-unit air conditioning systems (American Housing Survey, 2019), studies targeting lower-income households find lower rates of AC system operation due to the expense, or the use of undersized or inefficient systems that may not achieve sufficient cooling (Gronlund, 2014; Proctor et al., 1998).

It is important to note that, as summer cooling demands increase with rising summer temperatures, the decreasing reliability of the US electric grid (Fig. 1) is compounding the climate risk of intensifying heat exposure. In 2019, 34% of all major electric disruption events across the US occurred in the summer months of June, July, and August – a greater proportion of annual blackouts than during any other season. The average duration for summer blackout events categorized by the Energy Information Administration as “major” in 2019 was 20 h, with one event in Dallas, Texas leaving more than 500,000 customers without power for more than four days (USEIA, 2019). As the potential for concurrent heat wave and blackout events rises, urban governments and emergency managers are confronted with a pressing challenge to safeguard urban populations from heat-related illness (Sailor et al., 2019).

The intensity of building-interior temperatures estimated through this study well exceed national hazard thresholds for heat-related illness. Table 2 reports US National Weather Service heat index values – a metric responsive to both air temperature and relative humidity – for each residential structure type by time of day. All reported values fall into one of four health hazard classes, with average maximum heat index values indicating an elevated risk of heat stress and heat stroke for single-family structures (Extreme Caution and Danger categories). With almost 70% of all households residing in single-family structures (American Housing Survey, 2019), more than one million residents of Phoenix would be a risk of heat-related illness – including heat mortality – from a concurrent blackout and heat wave event of historical intensity.

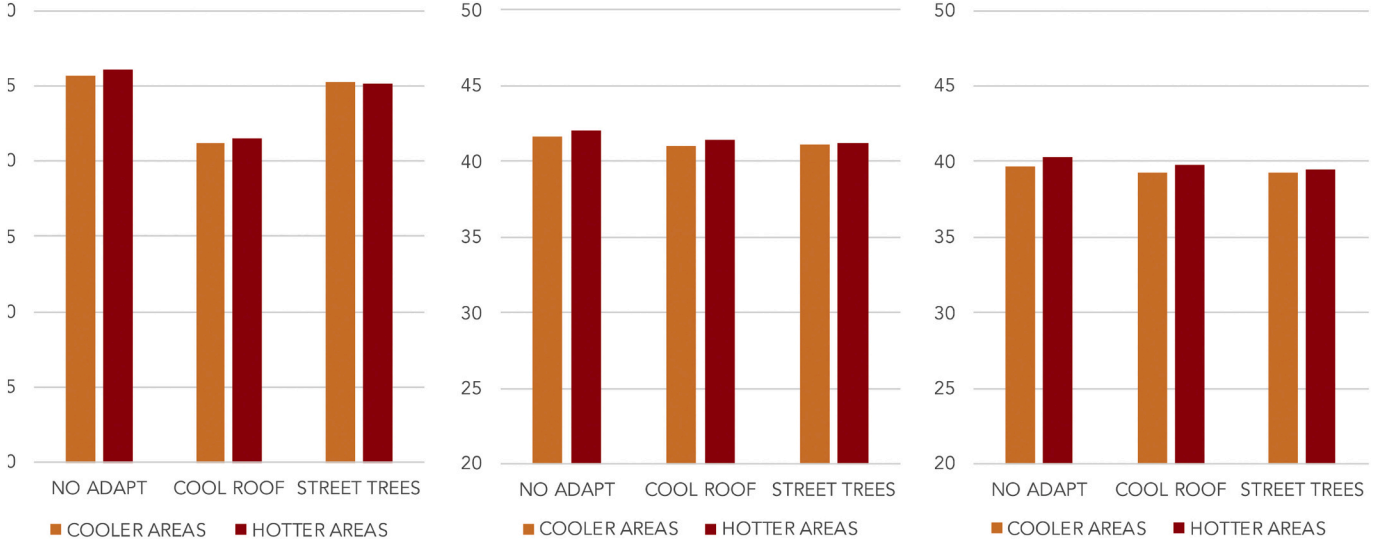

Fig. 6. Average maximum building-interior temperatures in hotter and cooler zones for 1-Story SF (left panel), 2-Story SF (middle panel), and Apartment (right panel) residential structures.

Table 1
Average ambient and building-interior temperatures for cooler (no shading) and hotter (gray shading) zones during July 20–24, 2006 under the BASE scenario. Hotter and cooler zones correspond to grid cells highlighted in Fig. 5.

	AMBIENT		1-STORY SF		2-STORY SF		APARTMENT	
DAY	44.8	47.2	45.7	46.1	41.6	42.1	39.7	40.3
NIGHT	31.4	32.9	32.4	33.2	33.3	33.8	32.0	33.0
DIURNAL RANGE	13.4	14.3	13.3	12.9	8.3	8.3	7.7	7.3
INDOOR MINUS AMBIENT DIURNAL RANGE			**-0.1**	**-1.4**	**-5.1**	**-6.0**	**-5.7**	**-7.0**

Table 2
Average maximum building-interior heat index values in Phoenix for July 20–24, 2006 by structure type. US National Weather Service Heat Index color coding: Extreme Danger (red); Danger (orange); Extreme Caution (yellow); Caution (beige).

STRUCTURE TYPE	TEMPERATURE	RELATIVE HUMIDITY	HEAT INDEX MAX
1-STORY SF	45.5ºC	6.9%	41ºC
2-STORY SF	41.5ºC	8.6%	38ºC
APARTMENT	39.6ºC	9.5%	36ºC

In addition to standard emergency response operations for heat wave events, including early warning systems and the provision of public cooling centers, we find that the installation of high-albedo cool roofs can yield health-protective benefits for residents lacking continuous access to mechanical air conditioning, and for all residents during blackout events. For the residential structure type most common in Phoenix – the single-story, single-family detached house – the installation of a cool roof was found to lower late afternoon indoor temperatures by 4.4 °C, a reduction sufficient to lower NWS heat risk class from Danger to Extreme Caution. This finding supports the prioritization of cool roof installation on residential structures with a high roof area-to-building volume ratio. A second urban heat management strategy, street tree planting, was found to yield only modest cooling benefits for building-interiors in Phoenix, although the direct effects of tree shading of residential structures were not captured in our analysis.

At present, few US cities have adopted cool roofing ordinances, and no US municipal ordinance or incentive program for cool roofing prioritizes residential buildings with a high roof area-to-building volume ratio. The City of Phoenix, for example, introduced a program in 2013 to install cool roofs on city-owned buildings but lacks any requirements for residential buildings. The establishment of minimum albedo and emissivity values for all residential roofs, as now required in Los Angeles, CA, would provide a minimum protective measure for the hazardous indoor heat exposures simulated through this work.

Part of an ongoing study of the growing heat risk posed by critical infrastructure failures in large US cities, the next phase of work will estimate heat-related mortality and morbidity among urban populations in response to concurrent heat wave and blackout events in the present and future time periods, as well as across the wider diversity of urban climates. In combination with this present study, this work is intended to inform a wide set of behavioral, environmental, and technological adaptations that can lessen the risk of extreme heat in cities during periods of prolonged power outages.

Supplementary data to this article can be found online at https://doi.org/10.1016/j.uclim.2021.100787.

Declaration of Competing Interest

The authors declare that they have no known competing financial interests or personal relationships that could have appeared to influence the work reported in this paper.

Acknowledgements

This material is based upon work supported by the National Science Foundation under Grant Number 1520803. Any opinions, findings, and conclusions or recommendations expressed in this material are those of the author(s) and do not necessarily reflect the views of the National Science Foundation.

References

American Housing Survey, 2019. US Census Bureau. Accessed online: April 20, 2020. https. www.census.gov/programs-surveys/ahs/data/interactive/ahstablecreator.html.

Anderson, G.B., Bell, M.L., 2012. Lights out: impact of the august 2003 power outage on mortality in New York, NY. Epidemiology 23 (2), 189.
Augenbroe, G., Brown, J., Heo, Y., Kim, S., Li, Z., McManus, S., Fei, Z., 2008. Lessons from an advanced building simulation course. In: Proceedings of the International Building Performance Simulation Association Conference, Berkeley, CA, pp. 261–268.
Berko, J., Ingram, D.D., Saha, S., Parker, J.D., 2004. Deaths attributed to heat, cold, and other weather events in the United States, 2006-2010. Natl. Health Stat. Rep. 76, 1–15.
Bierwagen, B.G., Theobald, D.M., Pyke, C.R., Choate, A., Groth, P., Thomas, J.V., Morefield, P., 2010. National housing and impervious surface scenarios for integrated climate impact assessments. Proc. Natl. Acad. Sci. 107 (49), 20887–20892.
Broadbent, A.M., Krayenhoff, E.S., Georgescu, M., 2020. Efficacy of cool roofs at reducing pedestrian-level air temperature during projected 21st century heatwaves in Atlanta, Detroit, and Phoenix (USA). Environ. Res. Lett. https://doi.org/10.1088/1748-9326/ab6a23.
Campbell, G., Norman, J., 1998. An Introduction to Environmental Biophysics. Springer.
Census Bureau, U.S., 2020. Quick Facts: Phoenix, Arizona. Accessed December 8, 2020. https://www.census.gov/quickfacts/phoenixcityarizona.
City of Phoenix, 2019. Mapping Open Data. https://mapping-phoenix.opendata.arcgis.com.
Crawley, D., Lawrie, L., Pedersen, C., Winkelmann, F., 2000. EnergyPlus: Energy simulation program. ASHRAE J. 42, 49–56.
Davis, R.E., Knappenberger, P.C., Michaels, P.J., Novicoff, W.M., 2003. Changing heat-related mortality in the United States. Environ. Health Perspect. 111, 1712–1718.
Dixon, P.G., Hedquist, B.C., Kalkstein, A.J., Goodrich, G.B., Walter, J.C., Dickerson, C.C., Penny, S.J., Cerveny, R.S., 2005. Heat mortality versus cold mortality: a study of conflicting databases in the United States. Bull. Am. Meteorol. Soc. 86, 937–943.
Georgescu, M., Morefield, P.E., Bierwagen, B.G., Weaver, C.P., 2014. Urban adaptation can roll back warming of emerging megapolitan regions. Proc. Natl. Acad. Sci. U. S. A. 111 (8), 2909–2914.
Goudriaan, J., 1977. Crop Micrometeorology: A Simulation Study. Simulation Monograph. PUDOC, Wageningen.
Gronlund, C., 2014. Racial and socioeconomic disparities in heat-related health effects and their mechanisms: a review. Curr. Epidemiol. Rep. 3, 165–173.
Habeeb, D., Vargo, J., Stone, B., 2015. Rising heat wave trends in large US cities. DOI. https://doi.org/10.1007/s11069-014-1563-z.
Hondula, D., Balling, R., Vanos, J., Georgescu, M., 2015. Rising temperatures, human health, and the role of adaptation. Curr. Clim. Change Rep. 1, 144–154.
Kovats, R.S., Hajat, S., 2008. Heat stress and public health: a critical review. Annu. Rev. Public Health 29, 41–55.
Krayenhoff, E.S., Christen, A., Martilli, A., Oke, T.R., 2014. A multi-layer radiation model for urban neighbourhoods with trees. Bound.-Layer Meteorol. 151 (1), 139–178.
Krayenhoff, E.S., Moustaoui, M., Broadbent, A.M., Gupta, V., Georgescu, M., 2018. Diurnal interaction between urban expansion, climate change and adaptation in US cities. Nat. Clim. Chang. 8 (12), 1097–1103.
Krayenhoff, E.S., Jiang, T., Christen, A., Martilli, A., Oke, T.R., Bailey, B.N., Nazarian, N., Voogt, J.A., Giometto, M.G., Stastny, A., Crawford, B.R., 2020. A multi-layer urban canopy meteorological model with trees (BEP-tree): street tree impacts on pedestrian- level climate. Urban Clim. 32, 100590.
Li, B., Duffield, C., Hutchinson, G., 2008. Simplified finite element Modelling of multi-storey buildings: the use of equivalent cubes. Electron. J. Struct. Eng. 8, 40–45.
Martilli, A., Clappier, A., Rotach, M.W., 2002. An urban surface exchange parameterisation for mesoscale models. Bound.-Layer Meteorol. 104 (2), 261–304.
Mendon, V., Lucas, R., Goel, S., 2013. Cost-Effective Analysis of the 2009 and 2012 IECC Residential Provisions – Technical Support Document. Pacific Northwest National Laboratory (Report #PNN- 22068).
Middel, A., Chhetri, N., Quay, R., 2015. Urban forestry and cool roofs: assessment of heat mitigation strategies in Phoenix residential neighborhoods. Urban For. Urban Green. 14 (1), 178–186.
National Center for Atmospheric Research (NCAR), 2016. European Centre for Medium- Range Weather Forecasts (ECMWF) ERA-Interim Project 2009. Accessed 29 November 2016. https://doi.org/10.5065/D6CR5RD9.
Parry, M.L., Canziani, O.F., Palutikof, J.P., Van der Linden, P.J., Hanson, C.E., 2007. Contribution of Working Group II to the Fourth Assessment Report of the Intergovernmental Panel on Climate Change. Cambridge University Press, Cambridge.
Patz, J.A., Campbell-Lendrum, Diarmid, Holloway, T., Foley, J.A., 2005. Impact of regional climate change on human health. Nature 438 (7066), 310–317.
Petkova, E.P., Gasparrini, A., Kinney, P.L., 2014. Heat and mortality in new York City since the beginning of the 20th century. Epidemiology 25 (4), 554–560.
Proctor, J., Huang, J., Lubiner, M., 1998. Monitored in-situ performance of residential air conditioning systems. ASHRAE Trans. 104, 1833–1840.
Rajput, M., Augenbroe, F., 2019. Heat stress in residential buildings as a result of deficient HVAC systems. In: Proceedings of the International Building Performance Simulation Association Conference, Rome, Italy, pp. 2482–2490.
Sailor, D.J., Baniassadi, A., O'Lenick, C.R., Wilhelmi, O.V., 2019. The growing threat of heat disasters. Environ. Res. Lett. 14 (5), 054006.
Santamouris, M., Ding, L., Fiorito, F., Oldfield, P., Osmond, P., Paolini, R., Prasad, D., Synnefa, A., 2017. Passive and active cooling for the outdoor built environment–analysis and assessment of the cooling potential of mitigation technologies using performance data from 220 large scale projects. Sol. Energy 154, 14–33.
Shindell, D., Zhang, Y., Scott, M., Ru, M., Stark, K., Ebi, K.L., 2020. The effects of heat exposure on human mortality throughout the United States. GeoHealth 3. https://doi.org/10.1029/2019GH000234 e2019GH000234.
Skamarock, W.C., Klemp, J.B., Dudhia, J., Gill, D.O., Barker, D.M., Duda, M.G., Huang, X.Y., Wang, W., Powers, J.G., 2008. A Description of the Advanced Research WRF Version 3 B. National Center for Atmospheric Research, CO, Editor, pp. 1–105.
Stone, B., Lanza, K., Mallen, E., Vargo, J., Russell, A., 2019. Urban heat management in Louisville, Kentucky: a framework for climate adaptation planning. J. Plan. Educ. Res. https://doi.org/10.1177/0739456X19879214.
US Department of Energy (USDOE), 2017. Residential Prototype Building Models, Building Codes Energy Program. https://www.energycodes.gov/development/residential/iecc_models.
US Energy Information Administration (USEIA), 2019. Annual Electric Power Industry Report, Form EIA-861 data files, October 2019. Accessed online April 20, 2020. https://www.eia.gov/electricity/data/eia861/.
US Environmental Protection Agency (USEPA), 2020. Energy Star Roof Product List. https://downloads.energystar.gov/bi/qplist/roofs_prod_list.pdf?8ddd-02cf.
Van Vliet, M.T.H., Yearsely, J.R., Ludwig, F., Vogele, S., Lettenmaier, D.P., Kabat, P., 2012. Vulnerability of US and European electricity supply to climate change. Nat. Clim. Chang. 2 (9), 676–681.